# Kinetic Model of Platinum Dissolution in PEMFCs

*Journal of The Electrochemical Society*, **150** (11) A1523-A1527 (2003)
0013-4651/2003/150(11)/A1523/5/$7.00 © The Electrochemical Society, Inc.



# Kinetic Model of Platinum Dissolution in PEMFCs

**Robert M. Darling*,z and Jeremy P. Meyers***

*UTC Fuel Cells, South Windsor, Connecticut 06074, USA*

This paper presents a mathematical model of oxidation and dissolution of supported platinum catalysts in polymer electrolyte membrane fuel cells (PEMFCs). Kinetic expressions for the oxidation and dissolution reactions are developed and compared to available experimental data. The model is used to investigate the influences of electrode potential and particle size on catalyst stability.

 [DOI: 10.1149/1.1613669] 

Manuscript submitted November 6, 2002; revised manuscript received April 30, 2003. Available electronically September 25, 2003.

The principle source of inefficiency in polymer electrolyte membrane fuel cells (PEMFCs) is sluggish oxygen-reduction reaction (ORR) kinetics at the cathode. Carbon-supported platinum catalyst is commonly used to enhance the rate of the ORR. In such catalysts, the high surface-to-volume ratio of the platinum particles maximizes the area of the surfaces available for reaction. If the platinum particles cannot maintain their structure over the lifetime of the fuel cell, changes in the morphology of the catalyst layer from the initial state results in a loss of electrochemical activity. It has been established experimentally that platinum dissolves in PEMFCs.[1,2] In this paper we develop a mathematical model for the kinetics of platinum dissolution and examine model predictions under a range of PEMFC operating conditions.

The model described in this paper is a spatially lumped model that treats a single, porous platinum electrode and the ionomeric solution that fills the pores of the electrode. The model includes spherical platinum particles that can grow and shrink as platinum plates and dissolves; a platinum oxide layer; and an ionic platinum species in solution ($Pt^{2+}$). This model contains the basic interfacial reactions and material balances, without including the mass-transport and reaction-rate distributions that come into play in a more detailed electrode model to be published later.

## Model Equations

*Electrochemistry*.—We consider three electrochemical reactions: platinum dissolution

$$Pt = Pt^{2+} + 2e^- \quad [1]$$

platinum oxide film formation

$$Pt + H_2O = PtO + 2H^+ + 2e^- \quad [2]$$

and chemical dissolution of platinum oxide

$$PtO + 2H^+ = Pt^{2+} + H_2O \quad [3]$$

In a purely thermodynamic analysis, one of these equations could be discarded; only two of them are thermodynamically independent. For example, Reaction 3 could be obtained by subtracting Reaction 2 from Reaction 1. However, we assume that the ion-exchange reaction, Reaction 3, occurs by a chemical pathway that is distinct from any combination of the two charge-transfer reactions; thus, it is included in the kinetic analysis of the system. $Pt^{2+}$ is assumed to be the only ionic platinum species present in significant amounts. Other ionic species with higher oxidation states are reported by Pourbaix,[3] but they are not expected to be important in the region of interest. In the literature the oxide species was often regarded to be $Pt(OH)_2$; however, recent quartz microbalance measurements show that the film is not hydrated.[4] This distinction is probably not critical in this work. Further oxidation of the PtO film is not considered explicitly in this work.

There are two methods by which we could lose platinum to the solution. The first is by the electrochemical dissolution of Pt to $Pt^{2+}$ according to Reaction 1, and the second is by the chemical dissolution of the PtO film according to Reaction 3. It is worth noting that the platinum dissolution reaction (Reaction 1) might be completely shut off, but the platinum particle size can still change through the combination of Reactions 2 and 3. Because the simulation tracks each reaction separately, it is possible to keep track of which reaction pathways are active for a given set of conditions, but from the point of view of observable changes to the system, the precise pathways are not so clearly identified. The forms of the rate expressions are somewhat arbitrary, but these forms are necessary to account for dissolution both from the bare platinum surface and from the oxide layer. It seems reasonable to have a simple expression for the dissolution of platinum to form the soluble species. If we are to retain that fairly simple expression for platinum dissolution from a bare platinum surface, then there must be two separate equations to describe platinum oxidation to form the oxide layer and to describe platinum dissolution from the oxide layer. Reaction 3 resembles the kinetics of a simple chemical equilibrium reaction.

*Rate equations*.—The platinum dissolution reaction is treated as a single elementary step. We propose a rate expression of the following form

$$r_1 = \frac{i_1}{n_1 F} = k_1 \theta_{vac} \left[ \exp\left( \frac{\alpha_{a,1} n_1 F}{RT} (\Phi_1 - \Phi_2 - U_1) \right) - \left( \frac{c_{Pt^{2+}}}{c_{Pt^{2+},ref}} \right) \exp\left( -\frac{\alpha_{c,1} n_1 F}{RT} (\Phi_1 - \Phi_2 - U_1) \right) \right] \quad [4]$$

where $\theta_{vac}$ is the fraction of the platinum surface that is not covered by oxides. This term is included in the forward rate expression to allow oxide on the surface to insulate the particle and prevent platinum dissolution from beneath the oxide film. $\theta_{vac}$ is included in the reverse term to prevent $Pt^{2+}$ from plating on Pt through a PtO film

$$U_1 = U_1^{\theta} - \frac{\Delta \mu_{Pt}}{2F} \quad [5]$$

Equation 5 is the standard equilibrium potential of Reaction 1. This potential is shifted away from the literature value for bulk platinum by the factor

$$\Delta \mu_{Pt} = \frac{\sigma_{Pt} M_{Pt}}{r \rho_{Pt}} \quad [6]$$

This factor accounts for the effect of the surface tension of the platinum crystallite on the equilibrium potential. As the platinum particle becomes larger, the shift in the chemical potential of platinum diminishes. The use of the Kelvin equation (Eq. 6) to describe the particle-size effect is likely a simplification and neglects the

* Electrochemical Society Active Member.
z E-mail: Robert.Darling@UTCFuelCells.com

energetics of multiple crystalline surface planes that likely exist on very small platinum particles. Such a formulation also neglects any specific interactions between the platinum surface and the electrochemical double layer.

The kinetic expression for platinum oxidation was adapted from the models of Harrington and Heyd,[4,5] and Conway and co-workers.[6] The anodic term, which describes the formation of the oxide, is equivalent to their models. The cathodic term was added in order to describe the reduction of PtO back to platinum metal. The original model of Conway and co-workers allows for unlimited growth of PtO on the Pt surface; our expression reaches equilibrium coverage when the forward and reverse rates are equal in magnitude. The equilibrium coverage may exceed a monolayer

$$r_2 = k_2\left[\exp\left(-\frac{\omega\theta_{PtO}}{RT}\right)\exp\left(\frac{\alpha_{a,2}n_2F}{RT}(\Phi_1 - \Phi_2 - U_2)\right) - \theta_{PtO}\left(\frac{c_{H^+}^2}{c_{H^+,ref}^2}\right)\exp\left(-\frac{\alpha_{c,2}n_2F}{RT}(\Phi_1 - \Phi_2 - U_2)\right)\right] \quad [7]$$

As in Reaction 1, the equilibrium potential for this reaction is shifted to account for the surface energy of the platinum crystallite. We also shifted the chemical potential of PtO from the value reported by Pourbaix.[3] In order to match the onset of platinum oxidation observed in cyclic voltammetry data, the platinum oxide must begin to form at lower potentials than would be predicted by using the chemical potential of bulk platinum oxide. Thus, one must assume that the oxide formed on the surface of a platinum crystallite is somehow stabilized by its interactions with the platinum metal and, hence, has a lower chemical potential than a bulk oxide. Alternatively, one might ascribe adsorption at low potentials to PtOH, which further oxidizes to PtO at higher potentials

$$U_2 = U_2^{\theta} + \frac{\Delta\mu_{PtO}}{2F} - \frac{\Delta\mu_{Pt}}{2F} \quad [8]$$

where

$$\Delta\mu_{PtO} = \Delta\mu_{PtO}^{0} + \frac{\sigma_{PtO}M_{PtO}}{r\rho_{PtO}} \quad [9]$$

$U_2$ may either increase or decrease with particle size depending upon the magnitudes of $\sigma_{Pt}$ and $\sigma_{PtO}$. The value of $\sigma_{Pt}$ used in this work exceeds the value of $\sigma_{PtO}$, which means that $U_2$ increases with particle size.

Finally, the rate of the chemical reaction is

$$r_3 = k_3\left(\theta_{PtO}c_{H^+}^2 - \frac{c_{Pt^{2+}}}{K_3}\right) \quad [10]$$

where the equilibrium constant, $K_3$, is again shifted from what one would calculate for bulk platinum oxide. This rate expression takes the form of a simple chemical equilibrium. The equilibrium constant, $K_3$, is related to $U_1$ and $U_2$ by the equation

$$K_3 = \exp\left[\frac{F}{RT}(n_1U_1 - n_2U_2)\right] \quad [11]$$

The proton concentration is related to the water content of the membrane material by the equation

$$c_{H^+} = \frac{1}{\frac{EW}{\rho_{Nafion}} + \frac{\lambda M_{H_2O}}{\rho_{H_2O}}} \quad [12]$$

where $M_{H_2O}$ is the molecular weight of water and $\lambda$ is the number of water molecules per acid site, and the concentration is defined as moles of protons per unit mass of water.

*Material balances*.—To complete the development of the mathematical model, we need an appropriate set of material balances. The kinetic equations involve five species: Pt, PtO, $Pt^{2+}$, $H^+$, and $H_2O$. We assume that the concentrations of protons and water are fixed and write material balances on the three remaining species. Assuming spherical platinum crystallites we get the following:

For PtO

$$\frac{d\theta_{PtO}}{dt} = \left(\frac{r_2 - r_3}{\Gamma_{max}}\right) - \left(\frac{2\theta_{PtO}}{r}\right)\frac{dr}{dt} \quad [13]$$

where $r$ is the particle radius and $\Gamma_{max}$ is the number of moles of active sites per unit of platinum area. This number is taken to be constant in this work and is calculated assuming a specific charge of 220 $\mu C/cm^2$ in the hydrogen adsorption region. This equation indicates that PtO grows as a film of uniform thickness, on the surface of the platinum crystallites.

For Pt we obtain

$$\frac{dr}{dt} = -\frac{M}{\rho}(r_1 + r_2) \quad [14]$$

where $M$ and $\rho$ are the molecular weight and density of platinum, respectively. Again, $r_1$ and $r_2$ refer to the reaction rates, in moles per second per square centimeter of Pt surface area.

Finally, a balance on $Pt^{2+}$ in solution yields

$$\varepsilon\frac{dc_{Pt^{2+}}}{dt} = 4\pi r^2N(r_1 + r_3) \quad [15]$$

where $\varepsilon$ is the porosity of the electrode, which is assumed to be constant. $N$ is the number of platinum crystallites per unit electrode volume

$$N = \frac{a}{4\pi r^2} \quad [16]$$

where a specific surface area of the electrode and $r$ is the mean particle radius measured after initial electrode formation, before cycling alters the particle-size distribution

The current density is

$$i = 8\pi r^2NFL(r_1 + r_2) \quad [17]$$

where $L$ is the thickness of the catalyst layer. Reaction 3 does not directly affect the current density because it is a chemical reaction, not an electrochemical reaction.

## Results and Discussion

Figure 1 shows an experimental cyclic voltammogram (CV) taken on a commercially available Gore 5510 membrane electrode assembly (MEA) and simulations run with the model described previously at a scan rate of 10 mV/s and a temperature of 50°C. Hydrogen adsorption on the platinum surface occurs below 0.4 V. This region of the voltammogram is used to measure the electrochemical area (ECA) of platinum catalysts. Between 0.4 and 0.6 V, no significant electrochemical reactions occur, and the response is dominated by the double-layer capacitance. Finally, above 0.6 V, platinum is oxidized. This is the region of interest in this work, as it corresponds to typical operating potentials in fuel cell cathodes. The goal of the modeling work is to fit parameters for Reactions 1-3 at typical cathode potentials. As stated previously, the dominant reaction is Reaction 2, platinum oxidation. Thus, the fit of the model to the experimental CVs is essentially determined by this reaction. However, platinum dissolution is the mechanism that we are ultimately interested in describing. The rate constant for the dissolution reaction was fit to unpublished data on changes in ECA caused by potential cycling experiments. The chemical dissolution of the platinum oxide film via Reaction 3 is more difficult to account for because it is not

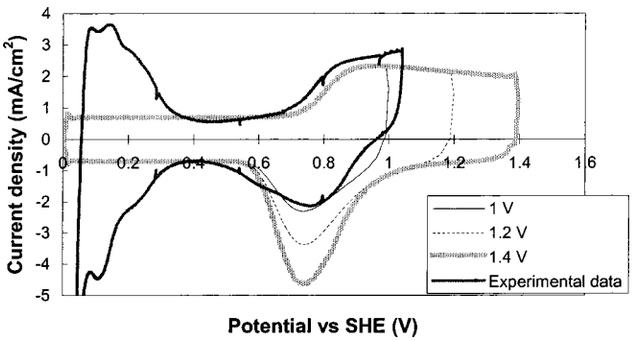


**Figure 1.** CVs of MEA with supported platinum catalyst to different upper potential sweep limits.

electrochemical, and so its rate cannot be determined by current measurements. Its rate was arbitrarily set to a low value.

The shape of the voltammogram at high potentials is unusual. On the anodic sweep there is a plateau beginning at approximately 0.85 V and extending to at least 1.5 V (not shown in this set of experimental data, but established in the literature). On the cathodic sweep there is a distinct peak centered at approximately 0.75 V. The long plateau on the anodic sweep happens because platinum oxide is not limited to monolayer coverage. Rather, multilayers of PtO may form. The onset of PtO formation predicted by the model, using the parameters in Table I, on the anodic sweep is approximately 25 mV too high. The location of the reduction peak predicted by the model matches the experiment, but the shape is different. The model particles discharge much of the film at a higher potential than what is observed experimentally. Table I lists the model parameters. Available literature values are given for comparison.

Figure 2 shows the surface coverage and platinum-ion concentration during the potential sweep experiments. The broad loops are the surface coverage, while the dashed lines are the $Pt^{2+}$ concentration. The surface coverage begins to increase rapidly at a potential of approximately 0.8 V and reaches values that vary from 0.6 at 1 V to 1.6 at 1.4 V. The maximum in surface concentration actually occurs after the sweep is reversed, because the reaction is slow. The system is not quick to come to equilibrium, and so for finite sweep rates, the oxide coverage is lower than the thermodynamic equilibrium coverage. Figure 3 clarifies this effect. Even as the potential sweep reverses and starts to decrease, the oxide coverage is in equilibrium with a lower potential. Eventually the decreasing potential and the lagging equilibrium potential cross, and the oxide layer is reduced.

**Table I. Fitting parameters.**

| Parameter | Fitted value | Literature value | Reference |
|---|---|---|---|
| $U_1^\theta$ | | 1.188 V | 3 |
| $\alpha_{a,1}$ | 0.5 | | Assumed |
| $\alpha_{c,1}$ | 0.5 | | Assumed |
| $k_1$ | $3.4 \times 10^{-13}$ mol/cm$^2$s | | Fitted |
| $U_2^\theta$ | | 0.98 V | 3 |
| $\alpha_{a,2}$ | 0.35 | 0.2-0.45 | 4 |
| $\alpha_{c,2}$ | 0.15 | | Fitted |
| $\omega$ | 30 kJ/mol | 24-35 kJ/mol | 4 |
| $\sigma_{Pt}$ | 0.237 mJ/cm$^2$ | 0.237 mJ/cm$^2$ | 7 |
| $\sigma_{PtO}$ | 0.1 mJ/cm$^2$ | 0.1 mJ/cm$^2$ | 7 |
| $\Delta\mu^0_{PtO}$ | −42.3 kJ/mol | | Fitted |
| $k_2$ | $1.36 \times 10^{-11}$ mol/cm$^2$s | | Fitted |
| $k_3$ | $3.2 \times 10^{-24}$ mol/cm$^2$s | | Assumed |
| $r$ | $3 \times 10^{-7}$ cm | | Observed |
| $C_{dl}$ | $7 \times 10^{-2}$ F/cm$^2$ | | Observed |

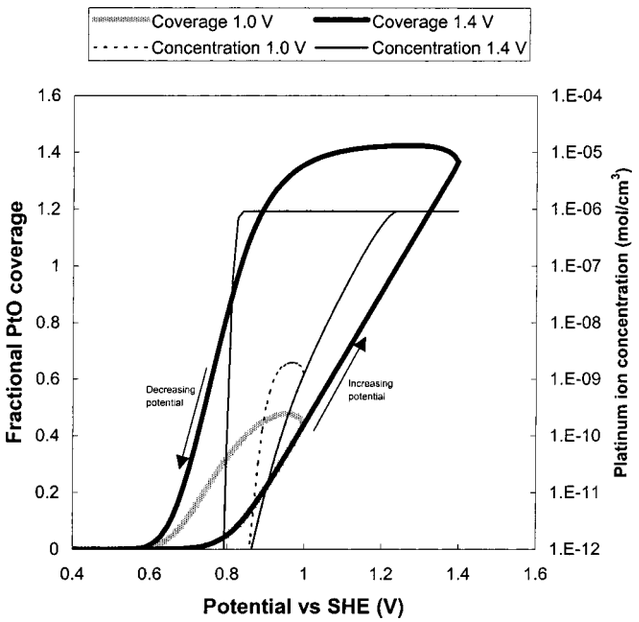


**Figure 2.** Oxide coverage and soluble platinum concentration during potential-sweep experiments.

The $Pt^{2+}$ concentration increases rapidly at 1.1 V, but it plateaus at a concentration of $7 \times 10^{-4}$ M, because at this sweep rate, it is at this concentration that the surface coverage of PtO reaches a monolayer, blocking off the surface from either further dissolution or plating. The $Pt^{2+}$ concentration drops on the reverse sweep once the PtO coverage falls below a monolayer and exposes the surface for platinum plating. The $Pt^{2+}$ is kinetically stable at the high potentials seen in this work, but it is not thermodynamically stable. Given enough time, the $Pt^{2+}$ would tend to convert to PtO chemically according to Reaction 3. We have assumed, however, that this reaction is slow.

Figure 4 shows the predicted equilibrium $Pt^{2+}$ concentration as a function of potential and temperature. The data of Bindra *et al.*[8] is included for the sake of comparison. The slope of the experimental data, taken in 96% $H_3PO_4$ at 176 and 196°C, agrees well with the simulations at 176°C. The simulations and experimental data are offset because temperature dependence of the standard equilibrium potentials was neglected due to a lack of experimental data on PtO. The slopes of the measured and simulated data below 1 V are consistent with the Nernst equation for Reaction 1. The solubility of

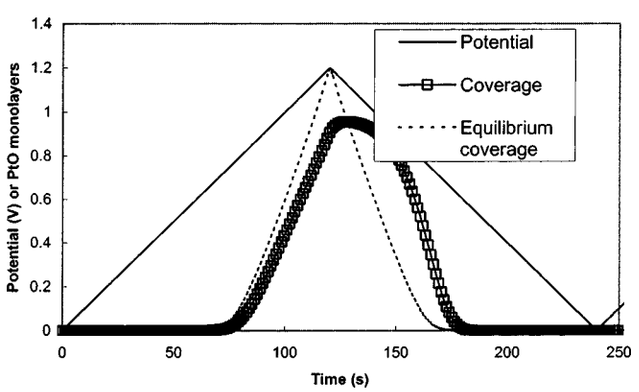


**Figure 3.** Comparison of equilibrium oxide coverage to predicted oxide coverage.

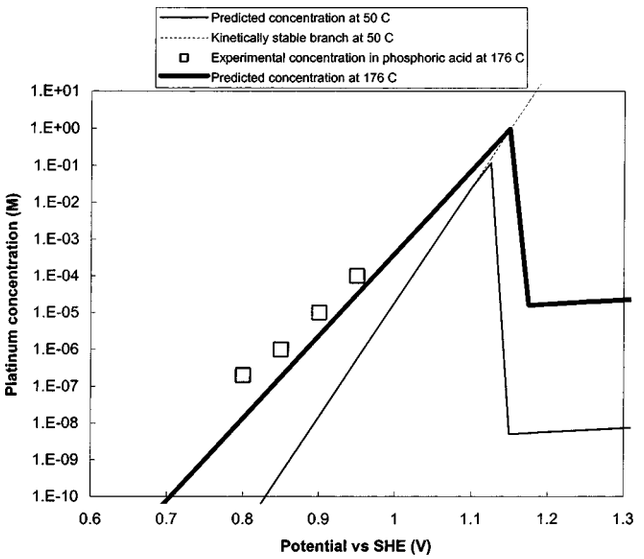


**Figure 4.** $Pt^{2+}$ concentration *vs.* potential.

platinum should be lower in a PEMFC than in a high-temperature fuel cell. The striking feature in the simulated data is the rapid drop in equilibrium concentration at approximately 1.1 V. At this point, the platinum surface is completely covered with platinum oxide, and the equilibrium is determined by Reactions 2 and 3. These simulations show the thermodynamic equilibrium concentrations (as defined by the three reactions), as well as the kinetically stable branch. As the sweeps proceed at higher sweep rates, the concentration of $Pt^{2+}$ in solution at more positive potentials can increase beyond the concentration in equilibrium with the PtO layer, as the Pt dissolution reaction continues as long as the surface is not completely covered. As stated previously, the rate of the chemical reaction was assumed to be slow for lack of better information. Thus, the approach to equilibrium at high potentials is slow.

This slow approach to equilibrium has a rather serious implication for Pt stability: Pt is stable at low potentials due to the low equilibrium concentration of $Pt^{2+}$ at these potentials, and Pt is fairly stable at higher potentials due to the protective oxide layer. Transitions between two potentials, however, can undermine the stability of the Pt crystallites, as the concentration of $Pt^{2+}$ in solution can increase by orders of magnitude over that which is stable at either low or high potentials. It is worth noting that this window of instability for a PEMFC occurs between the $H_2$-air open-circuit mixed potential at the cathode ($\sim$0.95 V) and the air-air open circuit potential ($\sim$1.229 V). Once the $Pt^{2+}$ dissolves into solution, it can be recaptured by the electrode from which it was liberated, but it can also diffuse to other regions of the MEA and permanently lower Pt content within the cathode. Thus, these transitions at start-up and shutdown can have profound implications on electrochemical area and performance of PEMFC cathodes.

Figure 5 compares, approximately, the platinum dissolution predictions of the model to the triangular-wave potential cycles of Kinoshita *et al.*[2] Kinoshita and co-workers measured platinum dissolution from sheet electrodes subjected to triangular cycles in 1 M $H_2SO_4$ at 23°C between 0.4 and 1.4 V at a rate of 1 cycle per minute and found an initial dissolution rate of 4.5 ng/cm$^2_{Pt}$-cycle.[a] This initial dissolution rate was determined by measuring the increase in soluble platinum concentration in a solution initially devoid of platinum species. The rate was essentially unchanged when the upper potential limit was dropped to 1.2 V, but the rate fell to approximately 0.8 ng/cm$^2_{Pt}$-cycle when the upper potential limit was dropped to 1.0 V. The model predicts initial dissolution rates of 0.5, 0.16, and $3.5 \times 10^{-4}$ ng/cm$^2_{Pt}$-cycle for these three cases, respectively. The measured dissolution rates at these potentials are approximately ten times the predicted rates at 1.2 and 1.4 V. The shapes of the experimental and simulated dissolution curves are similar The experimentally observed plateau in dissolution rate at high potentials appears to confirm the assumption that Reaction 3 is slow, because if Reaction 3 were rapid, then the dissolution rate would drop dramatically, as the PtO surface would rapidly equilibrate with the mobile platinum species in solution, rather than following the kinetic branch of the Pt dissolution reaction.

[a] The numbers reported in the text of Ref. 2 are 1000 times too large; the correct numbers may be determined from the figures.

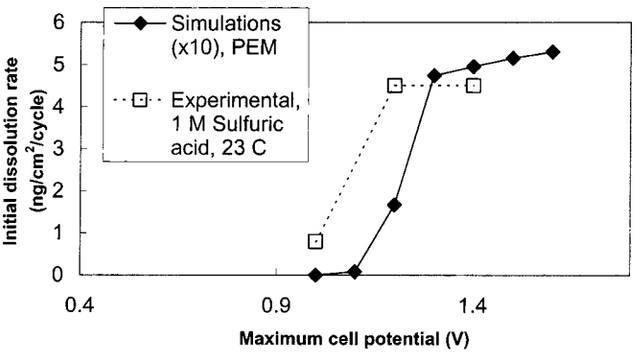


**Figure 5.** Initial dissolution rate *vs.* maximum cell potential for potential sweep experiments.

## Conclusions

The model presented in this document describes the oxidation and dissolution of platinum in a PEMFC. Parameters describing the oxidation of platinum were fit to CVs taken on commercially available supported platinum electrodes. The fit is reasonably good. The description of platinum oxidation differs from that proposed in the literature by the inclusion of the cathodic term, which is necessary to describe the reduction of platinum oxide to platinum. This leads to an equilibrium oxide coverage, which differs from the unlimited oxide growth predicted by the literature models. The platinum dissolution kinetics and solubility compare reasonably well with the data available in the literature.

## Acknowledgments

Thanks to M. Perry, T. Patterson, and J. A. S. Bett for their careful reviews of this document, and to UTC Fuel Cells for assistance with publication costs.

*UTC Fuel Cells assisted in meeting the publication costs of this article.*

## List of Symbols

| | |
|---|---|
| $c_i$ | concentration of species i, mol/cm$^3$ |
| $C_{dl}$ | double-layer capacitance, F/cm$^2$ |
| EW | equivalent weight of ionomer, g/acid equivalent |
| $F$ | Faraday's constant, 96,487 C/equiv |
| $i$ | current density, A/cm$^2$ |
| $k_i$ | rate constant for reaction i in the forward direction, mol/cm$^2$ s |
| $M$ | molecular weight of Pt, 195 g/mol |
| $M_{H_2O}$ | molecules weight of water, g/mol |
| $n_i$ | number of electrons in reaction i |
| $N$ | number of Pt particles per unit volume, cm$^{-3}$ |
| $r$ | particle radius, cm |
| $r_i$ | rate of reaction i, mol/cm$^2$ s |
| $R$ | universal gas constant, J/mol K |
| $t$ | time, s |
| $T$ | temperature, K |
| $U_i$ | thermodynamically reversible potential for reaction i, V |

Greek

- $\alpha_{a,i}$ anodic transfer coefficient for reaction i
- $\alpha_{c,i}$ cathodic transfer coefficient for reaction i
- $\beta_i$ symmetry coefficient for reaction i
- $\varepsilon$ electrode porosity
- $\Phi_1$ solid-phase potential, V
- $\Phi_2$ membrane-phase potential, V
- $\Gamma_{max}$ maximum surface coverage on platinum, $2.18 \times 10^{-9}$ mol/cm$^2$
- $\mu_i$ electrochemical potential of i, J/mol
- $\theta_{PtO}$ fraction of platinum surface covered by PtO
- $\theta_{vac}$ fraction of platinum surface not covered by PtO
- $\lambda$ water content of membrane, moles of water per equivalent of acid
- $\rho_{H_2O}$ density of water, g/cm$^3$
- $\rho_{Nafion}$ density of dry inomer, g/cm$^3$
- $\rho_{Pt}$ density of platinum, 21.0 g/cm$^3$
- $\rho_{PtO}$ density of platinum, 14.1 g/cm$^3$
- $\sigma_{Pt}$ surface tension, J/cm$^2$
- $\sigma_{PtO}$ surface tension, J/cm$^2$
- $\omega$ PtO-PtO interaction parameter, J/mol

## References


1. T. Patterson, in *Fuel Cell Technology Topical Conference Proceedings*, 2002 AIChE Spring National Meeting, March 10-14, 2002.
2. K. Kinoshita, J. T. Lundquist, and P. Stonehart, *J. Electroanal. Chem. Interfacial Electrochem.*, **48**, 157 (1973).
3. Marcel Pourbaix, *Atlas of Electrochemical Equilibria in Aqueous Solutions*, Pergamon Press, Oxford (1966).
4. D. V. Heyd and D. A. Harrington, *J. Electroanal. Chem.*, **335**, 19 (1992).
5. D. A. Harrington, *J. Electroanal. Chem.*, **420**, 101 (1997).
6. B. E. Conway, B. Barnett, H. Angerstein-Kozlowska, and B. V. Tilak, *J. Chem. Phys.*, **93**, 8361 (1990).
7. J. Bett, Personal communication.
8. P. Bindra, S. Clouser, and E. Yeager, *J. Electrochem. Soc.*, **126**, 1631 (1979).